

Received December 9, 2020, accepted December 28, 2020, date of publication January 14, 2021, date of current version February 1, 2021.

Digital Object Identifier 10.1109/ACCESS.2021.3051685

# Identification of Rice Varieties and Adulteration Using Gas Chromatography-Ion Mobility Spectrometry

XINGANG JU<sup>1,2,3,4</sup>, FEIYU LIAN<sup>2,4</sup>, HONGYI GE<sup>2,4</sup>, YUYING JIANG<sup>2,4</sup>, YUAN ZHANG<sup>1,2,4</sup>, AND DEGANG XU<sup>2,4</sup>

<sup>1</sup> Collaborative Innovation Center of Henan Grain Crops, Zhengzhou 450002, China

<sup>2</sup> Key Laboratory of Grain Information Processing and Control, Ministry of Education, Henan University of Technology, Zhengzhou 450000, China

<sup>3</sup> Key Discipline of Computer Software and Theory, School of Computer and Information Technology, Henan Finance University, Zhengzhou 450046, China

<sup>4</sup> Key Laboratory of Grain Photoelectric Detection and Control, Henan University of Technology, Zhengzhou 450000, China

Corresponding author: Yuan Zhang (zy\_haut@163.com)

This work was supported in part by the National Key Research and Development Program during the 13th Five-Year Plan Period under Grant 2017YFD0401003, and in part by the National Natural Science Foundation of China under Grant 61705061 and Grant 61975053.

**ABSTRACT** To solve the problems existing in traditional biochemical methods, such as complex sample pretreatment requirements, tedious detection processes and low detection accuracies with respect to rice species and adulteration, the volatile flavor substances of five kinds of rice are detected using headspace-gas chromatography-ion mobility spectrometry (HGC-IMS) to effectively identify the quality of rice and adulterated rice. The ion migration fingerprint spectra of five kinds of rice are identified using a semi-supervised generative adversarial network (SSGAN). We replace the output layer of the discriminator in a GAN with a softmax classifier, thus extending the GAN to a semi-supervised GAN. We define additional category tags for generated samples to guide the training process. Semi-supervised training is used to optimize the network parameters, and the trained discriminant network is used for classifying HGC-IMS images. The experimental results show that the prediction accuracy of the model reaches 98.00%, which is significantly higher than the rates achieved by other models, such as a decision tree, a support vector machine (SVM), improved SVM models (LS-SVM and PCA-SVM) and local geometric structure Fisher analysis (LGSFA); 98.00% is also higher than the prediction accuracies of the VGGNet, ResNet and Fast RCNN deep learning models. The experimental results also show that the accuracy of HGC-IMS image classification for identifying adulterated rice reaches 97.30%, which is higher than those of traditional chromatographic or spectral methods. The proposed method overcomes the shortcomings of some intelligent algorithms regarding the application of ion migration spectra and is feasible for accurately predicting rice varieties and adulterated rice.


**INDEX TERMS** Gas chromatography-ion migration spectrometry, ion migration fingerprint spectrometry, rice flavor substance, semi-supervised generated adversarial network.

## I. INTRODUCTION

Rice is a common staple food in Asia. Different kinds of rice have different flavors and tastes. For example, Thai fragrant rice contains a compound called acetyl-pyrroline (2-acetyl-1-pyrroline), which gives this rice a pleasant aroma, and Chinese Wuchang rice has an aroma, sweetness and good taste. These high-quality varieties of rice are usually expensive. To increase export income, a few distributors in Southeast

Asia often use Vietnamese or Cambodian rice as Thai fragrant rice (because these varieties have a similar appearance); in mainland China, rice is usually mixed, and other ordinary types of rice with similar appearances are used fraudulently. The use of Wuchang rice can increase profits. Therefore, determining the origin and variety of rice is very important in the grain market.

At present, rice quality is determined using sensory detection, electronic noses, chromatography, or spectroscopy. Sensory inspection is limited by the judgment and practical experience of the inspectors, and this leads to inconsistency.

The associate editor coordinating the review of this manuscript and approving it for publication was Vivek Kumar Sehgal .

Sensory inspection is generally only used for the preliminary determination of adulteration. As a new detection method, an electronic nose [1], [2] has shortcomings such as sensor drift, low accuracy, and poor consistency in its results, and its applications in the fields of food quality and safety inspection are unsatisfactory. Chromatography [3]–[6] has been used to detect adulterated rice, and it offers high efficiency, sensitivity, accuracy, and relative immunity to interference factors. However, due to the presence of different rice varieties and methods of processing rice (each rice variety has a unique composition of starch, protein, and fatty acids), using a chromatograph also has certain limitations. A chromatograph is a complicated piece of equipment that requires a professional operator, so it is not useful for rapid field detection. Although spectrometry [7]–[9] is fast and simple, it is difficult to accurately characterize the quality of samples with such techniques. Gas chromatography-mass spectrometry (GC-MS) is widely used in the field [10]–[12], but this method requires a sample to undergo pretreatment. GC-MS is used to search the library of mass spectrograms of unknown compounds for qualitative analysis. It has more advantages than chromatography, but there are still many shortcomings, such as the fact that compounds must be gasified, the operation is complex, and the maintenance of the equipment is expensive, all of which make it difficult for GC-MS to meet the requirements of the rapid detection market. Among the above methods, some (e.g., traditional spectroscopic methods) can be used for nondestructive testing, but their accuracies are low; some methods (e.g., conventional gas chromatography (GC), gas chromatography-mass spectrometry (GC-MS), and liquid chromatography-mass spectrometry (LC-MS)) have high accuracy, but they cannot perform detections quickly and nondestructively and require complex sample pretreatment processes [13], [14]. In recent years, high-performance liquid chromatography (HPLC) [15] and HPLC/MS [16], [17] have been used to detect and study rice, and some achievements have been produced. We also hope to find a simple, rapid, accurate and sensitive rice quality detection technology through our research. Spectroscopy is another available analysis technique; for example, hyperspectral images (HSIs) and local neighborhood structure-preserving embeddings for HSI classification (LNSPEs) could also be used. LNSPEs can effectively reveal the internal structure and improve the classification performance of HSI data [18]. Spatial-spectral hypergraph discriminant analysis (SSHGDA) has an advanced ability to distinguish features. The above methods can be used for detecting the spectral information of rice, combined with gas information discrimination [19].

Gas chromatography-ion migration spectrometry (GC-IMS) is a new gas phase separation and detection technology that has been used to evaluate the taste of white bread, the authenticity of ham [20] and the quality and authenticity of honey [21], [22]. GC-IMS is equipped with a static headspace sampling device, which can detect volatile organic compounds in liquid or solid samples and is suitable for trace detection of volatile organic compounds. This

technology combines the advantages of the fast response of gas chromatography and the high sensitivity of ion migration spectrometry, it is simple to operate, rapid and nondestructive, and it does not require sample pretreatment and has good reproducibility. This provides a new solution for rice adulteration and classification. At present, headspace-gas chromatography-ion mobility spectrometry (HS-GC-IMS) has been applied to the separation of volatile or semivolatile compounds.

However, the existing GC-IMS software only provides a simple principal component analysis (PCA) method for clustering. If determining the types of samples using the software is required, it is necessary to manually compare the fingerprints of the samples for classification. Due to the limitations of human experience and sensory perception, the method of distinguishing rice species directly from fingerprints leads to large classification errors and low efficiency. Therefore, it is necessary to adopt a machine learning method.

In spectrum analysis and recognition, the algorithms that can be used include traditional shallow neural networks (such as an SVM) and popular deep learning methods developed in recent years. Jacky Chan *et al.* [23] proposed a least squares support vector machine (LS-SVM) method to objectively assess Parkinson's disease with an accuracy rate of 96.0%. Lian *et al.* [24] used principal component analysis (PCA) to analyze genetically modified corn. The dimensionality reduction in the Hertz spectrum data and the classification using an SVM achieved good detection results, and the accuracy rate for the identified samples was close to 92.08%. Luo *et al.* [25] used PCA to reduce the dimensionality of hyperspectral images and the LGSFA algorithm to analyze a local geometric combination, and they achieved good classification results. In recent years, the development of convolutional neural networks has provided an opportunity to further improve spectral recognition rates. Yu *et al.* [26] found that VGGNet is the best model for detecting various broad-leaved weeds in dormant Bermuda. Chen Xuejing *et al.* [27] used ResNet to decode the Raman spectral-coded suspended array (SA) to obtain type information, and the classification accuracy of this method reached 100%. Ross Girshick [28] developed Fast RCNN in 2015, and this method greatly improved the speed of target detection. Li *et al.* [29] proposed a pedestrian and cyclist parallel detection algorithm based on Fast RCNN that was significantly better than other methods. The above algorithms have achieved good results in terms of the analysis and recognition of spectral data, but the recognition accuracy of the image spectrum obtained by a shallow neural network still needs to be improved, and a convolutional neural network needs a large number of training samples to achieve high accuracy. Due to these limiting conditions, we obtained fewer ion mobility spectrum samples than in previous studies, and we propose a semi-supervised GC-IMS fingerprint classification method based on a generative adversarial network [30]. Using a small number of labeled and unlabeled samples, the GAN discriminator network is used to output sample category labels and provide semi-supervised classification,

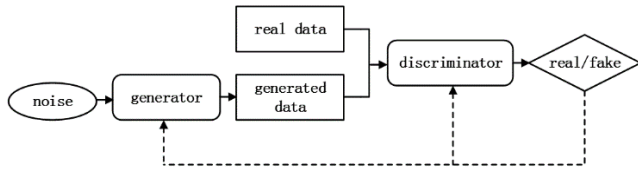


FIGURE 1. GAN flowchart.

thereby achieving the use of fewer labeled samples to improve the classification of the GC-IMS fingerprint spectrum.

II. MODELING METHOD

A classifier model can be used for automated rise identification from their gas phase ion migration spectra.

Many annotated natural image datasets have become available for use in deep learning and computer vision tasks. However, in practical problems, such as image classification, manually annotating specific images requires relevant professional knowledge. In addition, due to the restrictions of privacy, industry standards and the lack of information system integration, building large-scale professional image data and adding numerous annotations would undoubtedly consume considerable human and material resources. A small quantity of marked and unlabeled data can be used in this method. A GAN discriminator network is used to output data category labels, providing semi-supervised classification.

A. GAN

A GAN is a kind of unsupervised model based on game theory [31], [32] that was proposed by Goodfellow *et al.* in 2014. A flowchart showing the general GAN model is shown in Fig. 1. The model includes a generator G and discriminator D. G maps random noise with a certain distribution (such as a Gaussian or uniform distribution) to a target domain, and then the probability distribution of the real data is studied to generate samples G(z) that follow the distribution of the real data to the greatest extent possible [33]. Random noise can be used to avoid encountering the mode collapse problem. D determines whether the input sample is from the real dataset x or the generated dataset G(z), and a probability value D(•) for the real data is output [34]. The process of training a GAN is essentially to train the discriminator D and generator G. G is trained to maximize the probability of D making mistakes, and D is used to maximize the accuracy rate for discriminating between the real samples and generated samples [35]. Therefore, training G and D is a binary min-max game problem with the following objective function:

$$J^{(D)} = -E_{x \sim P_{data}(x)} \ln D(x) - E_{z \sim P_z(z)} [\ln(1 - D(G(z)))] \tag{1}$$

$$J^{(G)} = -E_{z \sim P_z(z)} [\ln D(G(z))] \tag{2}$$

where  $x \sim P_{data}(x)$  means that data x follows the  $P_{data}$  distribution, and  $z \sim P_z(z)$  means that the random noise z follows the distribution  $P_z$ .

During the training process for a GAN, the generator strives to make the generated pictures increasingly realistic

so that the discriminator cannot distinguish between the true and false images, and the goal of D is to try to distinguish real pictures from those produced by the network G. This process is similar to a two-player game, where G and D constitute a dynamic “game process.” As time goes by, the generator and the discriminator are constantly fighting, and finally, the two networks reach a dynamic balance: the image that G generates is close to the real image, and the discriminator cannot identify the true and false images. Therefore, the ultimate goal of network training is to ensure the maximization of the probability values of the G and D networks, and this objective is in fact to make G and D achieve “Nash equilibrium”.

B. SSGAN

The semi-supervised learning method used for a GAN is called an SSGAN. A semi-supervised GAN is an extension of the GAN architecture that is used to train classifier models and utilizes both labeled and unlabeled data. We attempt to use a semi-supervised GAN to classify GC-IMS images. For a class K classification problem, we use the newly generated class  $y = K + 1$  to label the generated image samples. Accordingly, the dimensions of the softmax classifier output are extended from K to K+1. In this way, the semi-supervised training method, which combines supervised loss with a loss function in an unsupervised GAN network [36], can provide increased accuracy in terms of semi-supervised classification by learning a large quantity of unlabeled sample data supplemented by a small quantity of labeled sample data [37]. The SSGAN network structure is shown in Fig. 2.

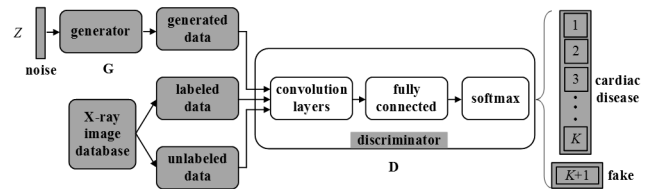


FIGURE 2. Framework of an SSGAN.

Noise Z conforming to a specific distribution is input into G to generate an image sample G(z) conforming to the distribution of the real data to the greatest extent possible. The generated image sample G(z) and the image sample library are input into D, where the database sample includes a small number of labeled samples and a large number of unlabeled samples. D is composed of multiple convolution layers and fully connected layers. At the beginning of the training process, neither the G loss nor D loss converges. Through continuous iterative training, G gradually fits the distribution of the image sample library to generate realistic image samples. Additionally, with the increase in the generated samples, D’s classification accuracy for input samples also increases.

To extract increasingly deep features and increase the stability of the training process, we constrain and adjust the network structures of G and D. For specific steps, we refer

to the literature [38], [39]. The specific adjustments are as follows: 1) convolution layers are used instead of pooling layers in D, and deconvolution layers are used instead of pooling layers in G; 2) batch normalization processing (batch norm) is used in D and G; 3) a tanh activation function is used in the output layer and the ReLU activation function is used in the remaining layers; 4) the LeakyReLU activation function is used in each layer in D [40], and the softmax function is used in the final output layer.

G uses a 5-layer deconvolution network to upsample random noise and generate simulation images with specific sizes. The network parameters are shown in Fig. 3. First, a 100-dimensional random noise vector  $Z$  is input into the fully connected network, which is then transformed into a three-dimensional tensor through dimension reduction. This tensor is input into the deconvolutional layer with a  $5 \times 5$  size and a stride length of 2 in the convolution kernel. Batch norm is executed each time deconvolution is performed. ReLU is used as the activation function for all other layers, except for the final output layer, which uses tanh activation. Finally, the output layer outputs a  $128 \times 128 \times 1$  tensor that is used to generate the image sample.

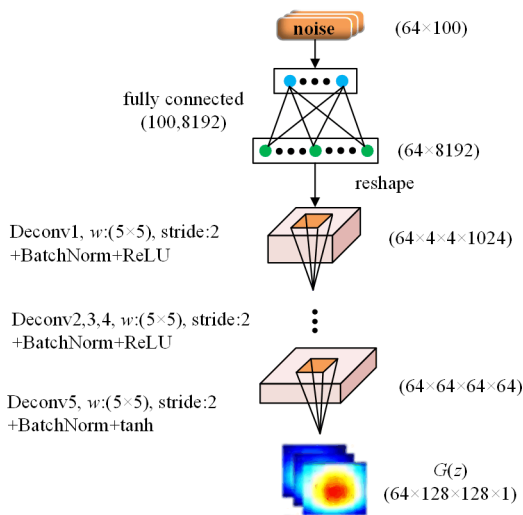


FIGURE 3. Generation network structure of the SSGAN.

D is composed of one convolutional layer and three fully connected layers, as shown in Fig. 4. The image samples are input into these convolutional layers with a  $3 \times 3$  convolution kernel. After each convolution, the batch norm operation is performed with LeakyReLU as the activation function. In contrast to the traditional ReLU activation function, LeakyReLU maintains a small slope on the negative half (a value of 0.2 is used in this paper) to keep the gradient from disappearing during training. Finally, a logic vector is output by the fully connected layer, and the category probability is normalized with the softmax output.

This network structure model is used to build a semi-supervised GC-IMS image classification algorithm. By combining supervised and unsupervised loss training methods

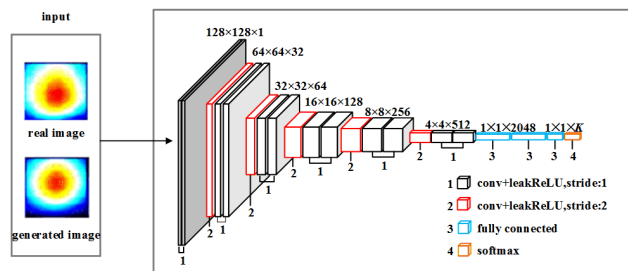


FIGURE 4. Structure of the discriminator D in our SSGAN.

to adjust the network parameters, common feature matching is used to increase the GAN's learning ability, as measured by its high image classification accuracy. When the model converges, the network is used to accurately classify GC-IMS images.

The specific training steps for the proposed SSGAN model are as follows:

- 1) Randomly sample a random vector  $z$  from the Gaussian distribution and input the random vector into the generator network G to obtain a simulated image  $G(z)$ .
- 2) Input the labeled or unlabeled real image  $x$  and the simulated image  $G(z)$  into the discriminator network D in batches, and output the normalized probability values  $D(x)$  and  $D[G(z)]$  using softmax.
- 3) Fixing the parameters of the generator network G, if the real image  $x$  is not labeled, use Lunlabel as the loss function; if the real image  $x$  is labeled, use Llabel as the loss function; and if the input image is a simulated image, use Lgen as the loss function. Use the Adam gradient descent method to adjust the parameters of the discriminator network D.
- 4) Fix the parameters of the discriminator network D, select the output of the fully connected layer as the middle layer feature, perform feature matching operations on the real image  $x$  and the simulated image  $G(z)$ , and adjust the parameters of the generator network G using feature matching.
- 5) Repeat steps 1)-4) until the desired number of iterations is reached.
- 6) Input the sample images into the discriminator D, and output the image category.

### III. INSTRUMENT AND EXPERIMENTS

#### A. INSTRUMENT

A diagram of our GC-IMS instrument is shown in Fig. 5. The IMS section introduces the molecular ion group into a region with an applied linear electric field. In the electric field, a constant velocity (migration rate) is obtained through collision with gas molecules drifting in reverse and a series of interactions, such as electric forces. IMS is similar to mass spectrometry, but deflection in mass spectrometry is governed by the charge-mass ratio ( $m/Z$ ), while deflection in IMS is dependent on ion mobility. Therefore, some isomers can be separated in IMS as long as they have different

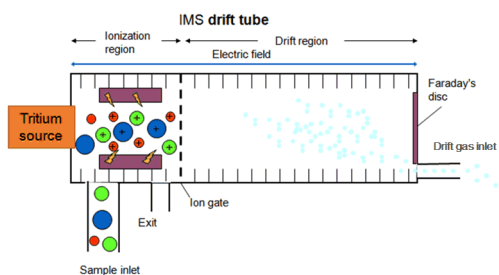


FIGURE 5. Working diagram of the GC-IMS instrument.

cross-sectional collision areas. The FlavourSpec<sup>®</sup> food flavor analysis and quality control system (G.A.S., Germany) was used in the experiment. Supporting analytical software was used to analyze samples from different angles. In the collected data, each point in the spectrogram represented a kind of volatile organic compound. A software plugin (Reporter) was used to directly compare the spectral differences between samples (2D and 3D views). Fingerprint spectra or differences in volatile organic compounds for different samples were compared with another plugin (Gallery Plot). Dynamic principal component analysis was used for sample clustering analysis and the rapid determination of unknown samples (Dynamic PCA plugin). The software included the NIST and IMS databases for qualitative analyses of substances (GC×IMS Library Search), and users can expand the database with data from standard substances. The sensitivity of the instrument was higher than the ppbv level, and the response time was 0.6 s.

### B. THE SAMPLES

Five rice samples were collected: Luodao 998 (ld998), Nanjing 9108 (nj9108), Zhenghan 10 (zh10), Liannuo 1 (ln1) and Baohan 1 (bh1). The samples were shelled and crushed, and 500 g powder samples were retained for each type of rice. These powder samples were separated into 100 samples for each type of rice, 70 of which were used for training the model and 30 were used for testing. In total, 500 samples from all five types of rice were used, of which 350 samples were used for training and 150 samples were used for testing. To compensate for the shortage of samples, the generated GC-IMS image samples from G were added to the dataset, so the training and testing sets were expanded to 3,500 and 1,500 samples, respectively.

### C. TEST CONDITIONS

By directly heating them after performing headspace injection, the volatile organic components in the rice sample can be quickly detected. The instrument can provide the sample gas phase ion migration spectra and a fingerprint chromatogram from volatile organic compounds, and this clearly shows the differences between the volatile components in each sample. This method is simple and rapid and can be used to identify the origins of rice varieties. The various parameters used for the analysis are shown in Table 1.

TABLE 1. Instrument parameters.

Parameter Settings for FlavourSpec <sup>®</sup>	
Analysis time	20 min
Column type	FS-SE-54-CB-1 15 m ID:0.53 mm
Column temperature	60°C
Carrier gas flow rate	0-2 min, 2 mL/min
	2-20 min, 2 mL/min-100 mL/min
Drift gas flow	150 mL/min
Carrier/drift gas	N <sub>2</sub>
IMS temperature	45 °C
Injection needle temperature	95 °C
Automatic headspace injection unit	
Sample volume	500 μL
Incubation time	15 min
Incubation temperature	90 °C

### D. TRAINING MODEL

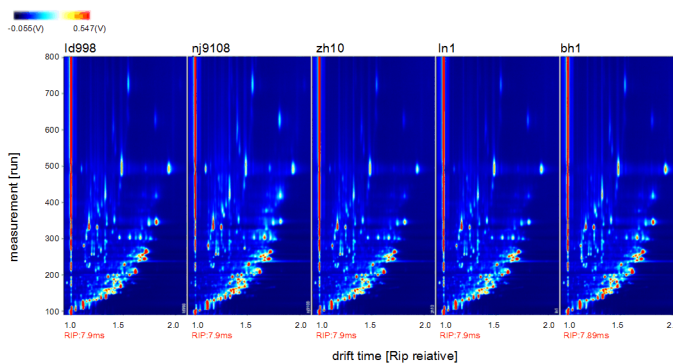
Supervised and unsupervised losses were used to adjust the network parameters in the discriminator to train the SSGAN model. Specifically, in the semi-supervised training process, D and G were trained alternately; either G or D was fixed, while the other's weight parameters were updated. When training and discriminating the networks, the network model parameters were updated by minimizing the cross-entropy loss of the labeled sample data and the probability distribution generated by the model. The principle of GAN confrontation training was used to adjust the real samples without labels and the network model parameters. When training the network, feature matching was used to ensure that the generated samples fit the distribution of the real data as closely as possible. The SSGAN network with semi-supervised classification ability was constructed using the above joint training method.

## IV. RESULTS AND DISCUSSION

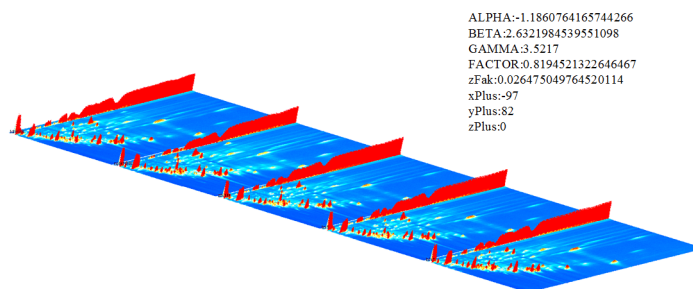
### A. GAS-ION MIGRATION SPECTRA OF SAMPLES

The samples (5 g) were placed in a 20 mL headspace sampling bottle, incubated at 90 °C for 15 min, and heated while they were oscillating. After 5 min, the aromatic components of the rice were uniformly released, and the samples were directly injected into the headspace (gas phase) for gas phase ion migration spectrum analysis. A headspace sampling analysis was conducted directly on the samples without the need for complex sample pretreatment, and the volatile components in the samples were determined after 20 min. The differences between the samples were quickly compared using software. The specific results are as follows:

Fig. 6(a) shows the GC-IMS spectra obtained from five rice samples, and Fig. 6(b) shows the corresponding stereogram. In Fig. 6(a), the vertical coordinate is the gas phase retention time, and the horizontal coordinate shows the ion drift time. The red vertical line on the left side of the plot denotes the reaction ion peak (RIP, approximately 7.9 ms of drift time after normalization). Each point on each side of the RIP represents a kind of volatile organic compound. The color represents the concentration of the substance, where white denotes less concentration, red means higher concentration,



(a)



(b)

FIGURE 6. Gas chromatography-ion mobility spectra of five rice samples.

and the darker the color is, the higher the concentration. As seen from the figure above, each type of rice has a different composition of volatile flavor substances.

**B. MANUAL QUALITATIVE ANALYSIS**

1) ESTABLISHING A STANDARD PRODUCT DATABASE

Prior to conducting a qualitative analysis, a database of ion migration spectra for volatile flavor compounds in grains should be established, namely, a corresponding database of the gas phase retention indices and migration times. The standard database can then be used to characterize the test results. To prevent the omission of volatile flavor compounds from testing, we referred to the partial ion migration spectrum data provided by the GCxIMS Library Search (G.A.S.). By testing the rice standards, we added relevant ion migration data for volatile flavor substances and produced the two-dimensional map for standard ion transport shown in Fig. 7, and the standard ion migration database is shown in Table 2. The test and application results show that the standard database contains almost all volatile flavor substances found in different varieties of rice, and this is suitable for a qualitative analysis of rice quality.

2) MANUAL QUALITATIVE ANALYSIS

Areas in the figure were selected for analysis, and fingerprint maps were generated, as shown in Fig. 8.

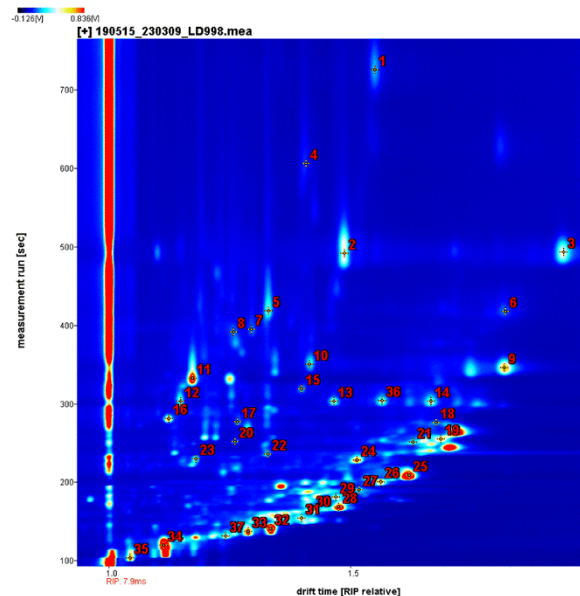


FIGURE 7. Ion migration profile of standard substances related to volatile flavor substances.

In Fig. 8, each pair of lines represents a sample containing signal peaks from all volatile organic compounds, and each column represents the signal from organic compounds (this refers to the same substance in different samples) with the same retention and drift times. One can see

**TABLE 2.** Volatile flavor substances shown in Fig. 7 and their ion migration parameters.

	Compound	CAS	Formula	MW	RI	Rt [s]	Dt [RIP rel]	Comment
1	Decanol	C112312	C10H20O	156.3	1257.1	724.717	1.551	
2	Nonanol	C124196	C9H18O	142.2	1106	491.678	1.4883	Monomer
3	Nonanol	C124196	C9H18O	142.2	1107.1	493.502	1.9419	Dimer
4	Octanoic Acid	C124072	C8H16O2	144.2	1179.9	605.652	1.4088	
5	(E)-2-octenal	C2548870	C8H14O	126.2	1058.1	418.591	1.3316	Monomer
6	(E)-2-octenal	C2548870	C8H14O	126.2	1057.3	417.486	1.822	Dimer
7	Phenylethyl alcohol	C60128	C8H10O	122.2	1041.3	394.28	1.2964	
8	Phenylacetaldehyde	C122781	C8H8O	120.2	1039.3	391.517	1.2598	
9	Octanol	C124130	C8H16O	128.2	1004.2	345.656	1.819	Dimer
10	Octanol	C124130	C8H16O	128.2	1007.9	350.076	1.4165	Monomer
11	2-Ethyl-6-methylpyrazine	C13925036	C7H10N2	122.2	992.5	332.395	1.1749	
12	Benzaldehyde	C100527	C7H6O	106.1	962.9	303.111	1.1501	Monomer
13	Benzaldehyde	C100527	C7H6O	106.1	962.9	303.111	1.4662	Dimer
14	(E)-2-heptenal	C18829555	C7H12O	112.2	962.3	302.558	1.6668	
15	3-Octanol	C589980	C8H18O	130.2	979.7	318.972	1.3993	
16	2,5-Dimethylpyrazine	C123320	C6H8N2	108.1	936.6	281.561	1.1252	
17	Ethyl pentanoate	C539822	C7H14O2	130.2	930.6	277.102	1.2679	Monomer
18	Ethyl pentanoate	C539822	C7H14O2	130.2	928.8	275.799	1.6787	Dimer
19	Heptanol	C111717	C7H14O	114.2	898.3	255.468	1.6871	
20	2-Heptanone	C110430	C7H14O	114.2	892.9	252.08	1.262	Monomer
21	2-Heptanone	C110430	C7H14O	114.2	890.3	250.516	1.6299	Dimer
22	1-Hexanol	C111273	C6H14O	102.2	865	235.919	1.3298	
23	(E)-2-hexanol	C928950	C6H12O	100.2	854.5	230.185	1.181	Monomer
24	(E)-2-hexanol	C928950	C6H12O	100.2	850.6	228.1	1.5144	Dimer
25	Butyl acetate	C123864	C6H12O2	116.2	811.7	208.551	1.6216	
26	Hexanol	C66251	C6H12O	100.2	794.9	200.731	1.5632	
27	1-Pentanol	C71410	C5H12O	88.1	770.8	190.045	1.5192	
28	Propyl acetate	C109604	C5H10O2	102.1	714.2	168.15	1.4763	
29	2-Methylbutanol	C137326	C5H12O	88.1	748	180.661	1.4715	
30	Pentanal	C110623	C5H10O	86.1	701.5	163.98	1.4215	
31	3-Methylbutanal	C590863	C5H10O	86.1	666.7	153.814	1.4001	
32	Ethyl acetate	C141786	C4H8O2	88.1	614.4	141.042	1.3358	
33	Isobutanol	C78842	C4H8O	72.1	598.3	137.393	1.2894	
34	Acetone	C67641	C3H6O	58.1	520.5	119.93	1.1143	
35	Ethanol	C64175	C2H6O	46.1	447.3	103.509	1.0453	
36	2-Pentyl-furan	C3777693	C9H14O	138.2	963.9	303.979	1.5658	
37	1-Propanol	C71238	C3H8O	60.1	573.2	131.764	1.2429	

from the figure that there are clear differences between the types of volatile component information in various samples. Fig. 8 also shows that the five kinds of rice contain roughly the same flavor substances, but the concentration of each substance is obviously different. Nonanal, octanal, heptanal, and pentanaldehyde (in the red frame in the figure) are most common in luodao998 and baohan1. The contents of caproaldehyde, E-2-octenal, and E-2-heptenal (in the green frame) in nanjing9108 are relatively high. Sample baoghan1 contains the highest contents of several kinds of acetic esters, such as ethyl acetate, propyl acetate, and butyl acetate (in the yellow frame). In addition, there is a characteristic substance in nanjing9108 that is marked “32” by the red arrow and

has a retention index of 926.5 and a migration time of 1.475. Through a search of the sample library, the substance may be 2-acetyl-1-pyrrolidine (consistent retention index, but we speculate that the substance has a ring structure based on its migration time), which is the main aromatic component in rice.

### C. ALGORITHM OF THE SSGAN MODEL

GC-IMS images were classified by running the SSGAN on a computer with a Tesla V100 GPU with 32 GB of video memory, a 4-core CPU, 32 GB of RAM, and 220 GB of disk space. A small number of labeled and unlabeled GC-IMS

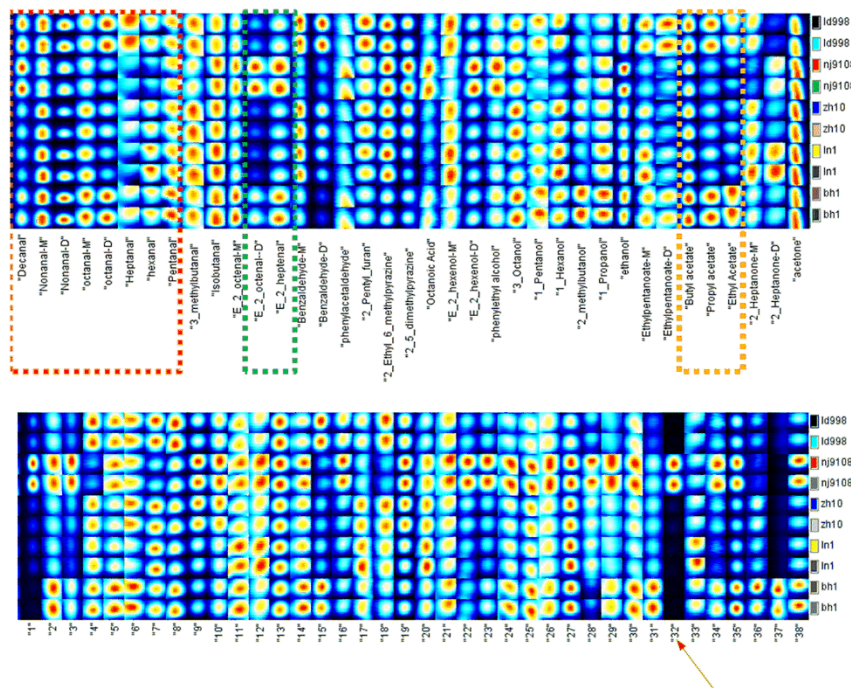


FIGURE 8. Ion migration fingerprints of the volatile organic compounds in Fig. 6.

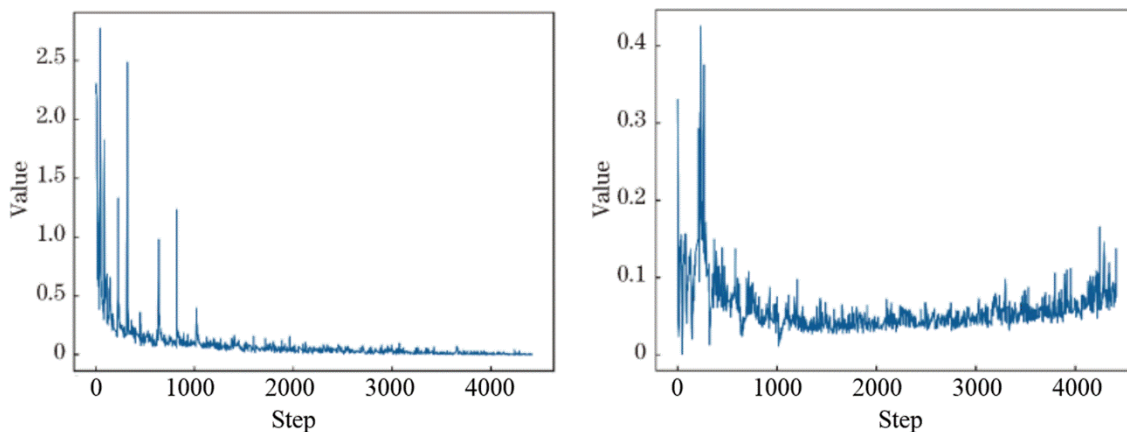


FIGURE 9. Loss function progress. (a) Discriminator network loss and (b) generator network loss.

sample images were classified. The loss function was optimized using the Adam algorithm. The learning rate was set to 0.0001, and the momentum was set to 0.5. Each group contained 64 samples. The changes in the loss function that occurred over successive iterations are shown in Fig. 9. In Fig. 9. (a), one can see that the network loss function oscillates during the early stage of training and eventually becomes relatively smooth. In Fig. 9. (b), the loss function in the generator network decreases rapidly and then rises slowly.

It should be noted that we did not consider the performance differences caused by mask changes because the image color and depth in this article were automatically generated by the software according to the types and concentrations of the volatile compounds.

The SSGAN was trained on a relatively small image dataset, and the algorithm was combined with a convolutional neural network (CNN) [41], the semi-supervised LadderNetwork (LadderNetwork) [10] and PCA+SVM [42]. Eight labeled datasets were defined with 25, 50, 100, 250, 500, and 1,000 labeled samples. Table 3 shows the average classification accuracies for the four corresponding algorithms with different numbers of labeled samples.

The experimental results show that the SSGAN requires fewer annotated data than the CNN. The SSGAN only requires 30 labeled samples to reach an accuracy of 61.367% ± 3.6%, while the CNN needs 50-250 labeled samples to reach the same accuracy level. In comparison with the other models, the SSGAN also achieves higher accuracy.



**TABLE 3. Average classification accuracies of models with different numbers of labeled samples.**

Labeled samples	Average accuracy/%			
	PCA+SVM	Ladder	CNN	SSGAN
10	51.62±4.5	52.02±6.3	47.36±4.1	57.58±6.1
30	57.83±5.2	56.59±3.2	54.51±5.1	61.36±3.6
50	62.19±3.9	63.27±2.6	60.53±4.4	67.69±3.2
100	67.73±4.5	71.68±5.3	70.67±4.2	76.85±4.1
250	71.89±6.1	75.26±4.3	77.21±4.5	79.96±5.9
500	74.32±7.2	77.40±4.1	82.36±6.5	84.31±5.3
1000	76.35±5.3	78.94±3.7	83.88±5.1	85.64±4.9

#### D. COMPARISON BETWEEN THE SSGAN AND OTHER MODELS

To verify the classification accuracy of the SSGAN model proposed in this paper, we compared it with an SVM, LS-SVM, PCA-SVM, and a decision tree model. A total of 350 samples were used for training the SSGAN. A total of 150 samples were used to train and test the SVM, LS-SVM, PCA-SVM, decision tree, and LGSFA models. A comparison of their prediction accuracies for the five rice species on the prediction set is shown in Table 4.

As shown in Table 4, the prediction accuracy of the SVM model improved when combined with PCA. The prediction accuracy provided by PCA-SVM was higher than that of the SVM, while the prediction accuracy of the SSGAN was the highest among all models, reaching 98.00%. The prediction accuracies of the other models listed in Table 4 varied greatly, but they all exhibited prediction accuracies less than 90%. In general, a comparison of the results from the five models clearly shows that the SSGAN provided a more accurate prediction than those of the other models.

To compare the recognition accuracy and time consumption of the SSGAN with those of some popular convolutional neural network methods developed in recent years, we selected VGGNet, ResNet and Fast RCNN for comparison experiments. The experimental environment settings were as follows: a Tesla V100 GPU with 32 GB of video memory, a 4-core CPU, 32 GB of RAM, 220 GB of disk space, and Python version 3.7.1. The network hyperparameters were set as follows: the input image size was 128\*128, the GPU was used to accelerate the training speed of the neural network, the adaptive moment estimation algorithm (Adam) was selected as the model parameter optimizer (optimizer), the learning rate (learning rate) was 0.001, and the loss function adopted cross-entropy loss (cross-entropy loss). The comparison results are shown in Table 5.

The SSGAN achieved an average accuracy of 98% in identifying various rice strains, and this was better than those of the three competing convolutional neural networks. This is because the SSGAN expands the data samples to improve recognition accuracy. Based on the time complexities of the algorithms, the time consumption of the SSGAN for identifying a sample did not increase significantly; it was only

slightly higher than that of Fast RCNN but better than those of the other convolutional neural networks, and the time achieved by the SSGAN can fully meet the requirements of practical applications.

#### E. COMPARISON BETWEEN HGC-IMS AND OTHER SPECTROMETRIC METHODS

To verify the classification accuracy of HGS-IMS for 5 kinds of rice, an electronic nose ( $\alpha$ -mos fox4000), gas chromatography-mass spectrometry (GC-MS), liquid chromatography-mass spectrometry (LC-MS), HPLC, and HPLC-MS were used to test the samples, and the data were used to form the training and test sets. The training and test sets contained the same quantities of data as described above. The aforementioned SSGAN model was constructed with the training set, and the test set was used for prediction. The prediction accuracy for the five rice species is shown in Table 6.

Table 6 shows that the data obtained with HGS-IMS produced the model with the highest prediction accuracy, indicating that GS-IMS can provide high-quality training data for use in a classification model. This also indicates that HGS-IMS, as a new organic volatile detection technology, has a higher material recognition rate and higher reliability than older methods.

#### F. IDENTIFICATION OF RICE ADULTERATION USING HGC-IMS

Rice adulteration identification refers to the identification of rice varieties that are different from the nominal variety (they may be other varieties of less important rice, indica rice, japonica rice, mold, mineral oil and artificial flavors) or do not contain the correct chemical rice components. It is estimated that 90% of Wuchang rice on the Chinese market is adulterated. The identification of adulterated rice is essentially a binary classification problem. If calculating the amount of adulterated rice is required, multiple regression analysis based on this method may be considered. Considering that the identification of adulteration is the most important aspect and that there are many types of volatile substances with different concentrations in rice, it is difficult to establish a multiple regression analysis model, so we did not conduct this research.

We define adulterated rice as positive and unadulterated rice as negative. The following indices were used to measure the identification performances of the models with respect to adulterated rice:

$$P = \frac{TP}{TP + FP} \quad (3)$$

$$R = \frac{TP}{TP + FN} \quad (4)$$

$$F1 = \frac{2 \times P \times R}{P + R} \quad (5)$$

$$A = \frac{TP + TN}{TP + TN + FP + FN} \quad (6)$$

TABLE 4. Prediction accuracies of various models.

Model	Total prediction accuracy	Prediction accuracy for each type of rice				
		ld998	nj9180	zh10	ln1	bh1
Decision Tree	76.00%	76.67%	73.33%	80.00%	73.33%	76.67%
SVM	82.67%	80.00%	83.33%	80.00%	86.67%	83.33%
LS-SVM	84.00%	83.33%	83.33%	86.67%	83.33%	83.33%
PCA-SVM	88.00%	86.67%	90.00%	86.67%	90.00%	86.67%
LGSFA	87.38%	87.01%	86.58%	86.71%	90.23%	86.35%
SSGAN	98.00%	94.00%	98.33%	99.67%	99.33%	98.67%

TABLE 5. Comparison between the prediction accuracies and running times of various deep learning algorithms.

Model	Training time/s	Total prediction accuracy	Prediction accuracy for each rice type				
			ld998	nj9180	zh10	ln1	bh1
VGGNet	0.23	89.01%	89.63%	88.67%	89.02%	89.22%	88.52%
ResNet	0.07	91.89%	91.00%	90.33%	93.00%	92.67%	92.43%
Fast RCNN	0.06	92.50%	92.91%	92.83%	93.77%	91.52%	91.49%
SSGAN	0.07	98.00%	94.00%	98.33%	99.67%	99.33%	98.67%

TABLE 6. Identification results of various methods.

Method	Total prediction accuracy	Prediction accuracy for each rice type				
		ld998	nj9180	zh10	ln1	bh1
Electronic Nose	55.67%	56.67%	50.00%	56.67%	60.55%	53.33%
GC-MS	72.00%	70.00%	73.33%	76.67%	73.33%	66.67%
LC-MS	74.00%	76.67%	70.00%	73.33%	73.33%	76.67%
HPLC	80.67%	80.00%	83.33%	80.00%	76.67%	83.33%
HPLC-MS	84.00%	83.33%	80.00%	86.67%	83.33%	86.67%
GC-IMS	98.00%	94.00%	98.33%	99.67%	99.33%	98.67%

TABLE 7. Confusion matrix of five kinds of rice.

Confusion matrices	Actual value					
	ld998	nj9180	zh10	ln1	bh1	
ld998	28	0	0	0	0	
nj9180	0	29	0	1	0	
Predicted value	zh10	1	1	30	0	0
	ln1	0	0	0	29	0
	bh1	1	0	0	0	30

Among them, *TP* and *FP* are the number of true positive samples that were correctly and incorrectly identified, while *TN* and *FN* represent the number of true negative samples that were correctly and incorrectly identified, respectively. *P* (precision) corresponds to the proportion of real positive samples

that made up the total number of predicted positive samples. *R* (recall) refers to the number of positive examples in the sample that were predicted correctly. *F1* is a harmonic mean based on precision and recall. A larger value of *F1* denotes higher accuracy. *A* (accuracy) is the accuracy rate. When the classification problem is a multipoint problem, by formula (6), the confusion matrix can list its accuracy rate; see Table 7.

Wuchang Daohuaxiang rice was taken as an example to identify adulteration. Fifty-eight rice samples labeled “Wuchang Daohuaxiang” were obtained from a market. Through a manual and scientific analysis, 37 cases were found to be positive, and 21 were found to be negative. There were 42 samples of homemade-adulterated Wuchang Daohuaxiang rice, including 13 positive samples and 29 negative samples, for a total of 100 samples (50 positive and 50 negative samples). The dataset was divided into training and test

**TABLE 8.** Binary classification results for the adulterated rice samples gathered with each method.

Method	Training set			Test set		
	Precision	Recall	F1	Precision	Recall	F1
Electronic Nose	0.545	0.514	0.529	0.573	0.533	0.533
GC-MS	0.645	0.571	0.606	0.688	0.733	0.709
LC-MS	0.655	0.543	0.593	0.667	0.667	0.667
HPLC	0.800	0.800	0.800	0.750	0.800	0.774
HPLC-MS	0.857	0.857	0.857	0.867	0.867	0.867
GC-IMS	0.917	0.943	0.930	0.973	0.973	0.973

**TABLE 9.** confusion matrix of wuchang rice adulteration.

Confusion matrices		Actual value	
		Wuchang	Non-Wuchang
Predicted value	Wuchang	49	1
	Non-Wuchang	1	49

sets, among which 70 were training samples and 30 were test samples. The numbers of positive and negative samples were equal. Using the above sample sets, we compared the performances of some conventional methods and the GC-IMS method in terms of rice adulteration identification. The classification results obtained by the various methods discussed in this paper are shown in Table 8.

Table 6 shows that GC-IMS provided sample data that achieved the highest classification accuracy according to all three indicators, followed by HPLC-MS and HPLC; the electronic nose had the lowest accuracy and F1 value. The F1 value of GC-IMS reached 0.973, an increase of 10.6% over the current best HPLC-MS method. A confusion matrix can be used to express the accuracy of the dichotomous problem by formula (3); see Table 9.

In addition, because the GC-IMS method greatly simplifies the sample preprocessing procedure, an intelligent prediction model not only improved the prediction accuracy but also greatly reduced the classification time. It is estimated that using GC-IMS and the model proposed in this paper could provide 50%-70% higher detection efficiency than existing methods when examining rice strains and adulteration.

## V. CONCLUSION

In this article, combined with an improved GAN algorithm (SSGAN), we used GC-IMS technology to identify five types of rice and rice adulteration. We used a small number of labeled samples and a large number of unlabeled samples generated by the GAN and used a semi-supervised learning method to train an improved SSGAN model. The recognition accuracy of the model for the five species of rice reached 98.00% on the test set, and the recognition accuracy with respect to adulterated rice reached 97.30%. We compared the SSGAN model with the popular VGGNet network, ResNet and other networks, and the results showed that the

recognition performance of the SSGAN was better than those of these alternative models. We also compared the method in this paper with other commonly used detection methods, such as HPLC, and the results showed that the recognition method of GC-IMS combined with the SSGAN proposed in this paper is superior to the existing biochemical methods in terms of recognition performance. Of course, the ultimate goal of the model is to identify sample types without labels, so we applied the model to real rice quality supervision and achieved good recognition results based on the users' feedback. In short, GC-IMS combined with the SSGAN can effectively identify rice species and adulteration. In future work, we will apply this method to the identification of other food crops.

## ACKNOWLEDGMENT

The authors would like to thank Jizhi Wan, a sales engineer at Hanong Company, Zhengzhou, China, who helped them with some experiments.

## REFERENCES

- [1] S. Gu, J. Wang, and Y. Wang, "Early discrimination and growth tracking of aspergillus spp. Contamination in rice kernels using electronic nose," *Food Chem.*, vol. 292, pp. 325–335, Sep. 2019, doi: 10.1016/j.foodchem.2019.04.054.
- [2] H. Rahimzadeh, M. Sadeghi, M. Ghasemi-Varnamkhasi, S. A. Mireei, and M. Tohidi, "On the feasibility of metal oxide gas sensor based electronic nose software modification to characterize rice ageing during storage," *J. Food Eng.*, vol. 245, pp. 1–10, Mar. 2019, doi: 10.1016/j.jfoodeng.2018.10.001.
- [3] H. Takagi, S. Suzuki, and S. Kitamura, "Selective adsorption of essential oil compounds by Waxy/Amylose extender (wx/ae) double-mutant rice starch revealed by gas chromatography," *Starch Stärke*, vol. 71, nos. 1–2, Jan. 2019, Art. no. 1700301, doi: 10.1002/star.201700301.
- [4] C. Sun, L. Zeng, J. Xu, L. Zhong, X. Han, L. Chen, Y. Zhang, and D. Hu, "Residual level of dimethachlon in rice-paddy field system and cooked rice determined by gas chromatography with electron capture detector," *Biomed. Chromatography*, vol. 32, no. 7, p. e4226, Jul. 2018, doi: 10.1002/bmc.4226.
- [5] L. Zhang, R. Yu, Y. Yu, C. Wang, and D. Zhang, "Determination of four acetanilide herbicides in brown rice juice by ionic liquid/ionic liquid-homogeneous liquid-liquid micro-extraction high performance liquid chromatography," *Microchem. J.*, vol. 146, pp. 115–120, May 2019, doi: 10.1016/j.microc.2018.12.062.
- [6] W. Setyaningsih, I. E. Saputro, C. A. Carrera, M. Palma, and C. García-Barroso, "Fast determination of phenolic compounds in rice grains by ultraperformance liquid chromatography coupled to photodiode array detection: Method development and validation," *J. Agricult. Food Chem.*, vol. 67, no. 10, pp. 3018–3027, Mar. 2019, doi: 10.1021/acs.jafc.8b05430.

- [7] J. Chen, M. Li, T. Pan, L. Pang, L. Yao, and J. Zhang, "Rapid and non-destructive analysis for the identification of multi-grain rice seeds with near-infrared spectroscopy," *Spectrochimica Acta A, Mol. Biomol. Spectrosc.*, vol. 219, pp. 179–185, Aug. 2019, doi: [10.1016/j.saa.2019.03.105](https://doi.org/10.1016/j.saa.2019.03.105).
- [8] Z. Ozbekova and A. Kulmyrzaev, "Study of moisture content and water activity of rice using fluorescence spectroscopy and multivariate analysis," *Spectrochimica Acta A, Mol. Biomol. Spectrosc.*, vol. 223, Dec. 2019, Art. no. 117357, doi: [10.1016/j.saa.2019.117357](https://doi.org/10.1016/j.saa.2019.117357).
- [9] Q. Zuo, Y. Chen, Z.-P. Chen, and R.-Q. Yu, "Quantification of cadmium in rice by surface-enhanced Raman spectroscopy based on a ratiometric indicator and conical holed enhancing substrates," *Anal. Sci.*, vol. 34, no. 12, pp. 1405–1410, Dec. 2018, doi: [10.2116/analsci.18P342](https://doi.org/10.2116/analsci.18P342).
- [10] P. J. Heinsvig, L. S. Nielsen, and C. Lindholm, "Development of a method using gas chromatography–mass spectrometry for profiling of oil-based androgenic anabolic steroid products," *J. Chromatography A*, vol. 1620, Jun. 2020, Art. no. 460989, doi: [10.1016/j.chroma.2020.460989](https://doi.org/10.1016/j.chroma.2020.460989).
- [11] S. Choi, H.-S. Seo, K. R. Lee, S. Lee, J. Lee, and J. Lee, "Effect of milling and long-term storage on volatiles of black rice (*Oryza sativa* L.) determined by headspace solid-phase microextraction with gas chromatography–mass spectrometry," *Food Chem.*, vol. 276, pp. 572–582, Mar. 2019, doi: [10.1016/j.foodchem.2018.10.052](https://doi.org/10.1016/j.foodchem.2018.10.052).
- [12] Y. J. Park, S. U. Park, S.-H. Ha, S. H. Lim, and J. K. Kim, "Improved quantification of  $\alpha$ -aminobutyric acid in rice using stable isotope dilution gas chromatography–mass spectrometry," *Food Chem.*, vol. 266, pp. 375–380, Nov. 2018, doi: [10.1016/j.foodchem.2018.06.036](https://doi.org/10.1016/j.foodchem.2018.06.036).
- [13] Z. Yang, R. Nakabayashi, T. Mori, S. Takamatsu, S. Kitanaka, and K. Saito, "Metabolome analysis of *oryza sativa* (Rice) using liquid chromatography–mass spectrometry for characterizing organ specificity of flavonoids with anti-inflammatory and anti-oxidant activity," *Chem. Pharmaceutical Bull.*, vol. 64, no. 7, pp. 952–956, 2016, doi: [10.1248/cpb.c16-00180](https://doi.org/10.1248/cpb.c16-00180).
- [14] Y.-X. Fang, H.-P. Song, J.-X. Liang, P. Li, and H. Yang, "Rapid screening of pancreatic lipase inhibitors from *monascus*-fermented rice by ultrafiltration liquid chromatography–mass spectrometry," *Anal. Methods*, vol. 9, no. 23, pp. 3422–3429, 2017, doi: [10.1039/C7AY00777A](https://doi.org/10.1039/C7AY00777A).
- [15] A. Sabir, M. Rafi, and L. K. Darusman, "Discrimination of red and white rice bran from Indonesia using HPLC fingerprint analysis combined with chemometrics," *Food Chem.*, vol. 221, pp. 1717–1722, Apr. 2017, doi: [10.1016/j.foodchem.2016.10.114](https://doi.org/10.1016/j.foodchem.2016.10.114).
- [16] W. Jira and S. Mánch, "A sensitive HPLC-MS/MS screening method for the simultaneous detection of barley, maize, oats, rice, rye and wheat proteins in meat products," *Food Chem.*, vol. 275, pp. 214–223, Mar. 2019, doi: [10.1016/j.foodchem.2018.09.041](https://doi.org/10.1016/j.foodchem.2018.09.041).
- [17] W. Li, Y. Zhang, H. Jia, W. Zhou, B. Li, and H. Huang, "Residue analysis of tetraniliprole in rice and related environmental samples by HPLC/MS," *Microchem. J.*, vol. 150, Nov. 2019, Art. no. 104168, doi: [10.1016/j.microc.2019.104168](https://doi.org/10.1016/j.microc.2019.104168).
- [18] G. Shi, H. Huang, and L. Wang, "Unsupervised dimensionality reduction for hyperspectral imagery via local geometric structure feature learning," *IEEE Geosci. Remote Sens. Lett.*, vol. 17, no. 8, pp. 1425–1429, Aug. 2019, doi: [10.1109/LGRS.2019.2944970](https://doi.org/10.1109/LGRS.2019.2944970).
- [19] F. Luo, B. Du, L. Zhang, L. Zhang, and D. Tao, "Feature learning using spatial-spectral hypergraph discriminant analysis for hyperspectral image," *IEEE Trans. Cybern.*, vol. 49, no. 7, pp. 2406–2419, Jul. 2019, doi: [10.1109/TCYB.2018.2810806](https://doi.org/10.1109/TCYB.2018.2810806).
- [20] D. Pu, H. Zhang, Y. Zhang, B. Sun, F. Ren, H. Chen, and J. He, "Characterization of the aroma release and perception of white bread during oral processing by gas chromatography-ion mobility spectrometry and temporal dominance of sensations analysis," *Food Res. Int.*, vol. 123, pp. 612–622, Sep. 2019, doi: [10.1016/j.foodres.2019.05.016](https://doi.org/10.1016/j.foodres.2019.05.016).
- [21] X. Wang, S. Yang, J. He, L. Chen, J. Zhang, Y. Jin, J. Zhou, and Y. Zhang, "A green triple-locked strategy based on volatile-compound imaging, chemometrics, and markers to discriminate winter honey and sapium honey using headspace gas chromatography-ion mobility spectrometry," *Food Res. Int.*, vol. 119, pp. 960–967, May 2019, doi: [10.1016/j.foodres.2019.01.004](https://doi.org/10.1016/j.foodres.2019.01.004).
- [22] N. Gerhardt, M. Birkenmeier, S. Schwolow, S. Rohn, and P. Weller, "Volatile-compound fingerprinting by Headspace-Gas-Chromatography ion-mobility spectrometry (HS-GC-IMS) as a benchtop alternative to <sup>1</sup>H NMR profiling for assessment of the authenticity of honey," *Anal. Chem.*, vol. 90, no. 3, pp. 1777–1785, Feb. 2018, doi: [10.1021/acs.analchem.7b03748](https://doi.org/10.1021/acs.analchem.7b03748).
- [23] J. Chan, H. Leung, and H. Poizner, "Correlation among joint motions allows classification of parkinsonian versus normal 3-D reaching," *IEEE Trans. Neural Syst. Rehabil. Eng.*, vol. 18, no. 2, pp. 142–149, Apr. 2010, doi: [10.1109/TNSRE.2009.2023296](https://doi.org/10.1109/TNSRE.2009.2023296).
- [24] F. Y. Lian, D. G. Xu, M. X. ., H. Y. Fu Ge, Y. Y. Jiang, and Y. Zhang, "Identification of Transgenic Ingredients in Maize Using Terahertz Spectra," *IEEE Trans. Terahertz Sci. Technol.*, pp. 1–7, vol. 2017, doi: [10.1109/TTHZ.2017.2708983](https://doi.org/10.1109/TTHZ.2017.2708983).
- [25] F. Luo, H. Huang, Y. Duan, J. Liu, and Y. Liao, "Local geometric structure feature for dimensionality reduction of hyperspectral imagery," *Remote Sens.*, vol. 9, no. 8, p. 790, Aug. 2017, doi: [10.3390/rs9080790](https://doi.org/10.3390/rs9080790).
- [26] J. Yu, S. M. Sharpe, A. W. Schumann, and N. S. Boyd, "Detection of broadleaf weeds growing in turfgrass with convolutional neural networks," *Pest Manage. Sci.*, vol. 75, no. 8, pp. 2211–2218, Aug. 2019.
- [27] X. Chen, L. Xie, Y. He, T. Guan, X. Zhou, B. Wang, G. Feng, H. Yu, and Y. Ji, "Fast and accurate decoding of Raman spectra-encoded suspension arrays using deep learning," *Analyst*, vol. 144, no. 14, pp. 4312–4319, Jul. 2019, doi: [10.1039/C9AN00913B](https://doi.org/10.1039/C9AN00913B).
- [28] R. Girshick, "Fast R-CNN," in *Proc. IEEE Int. Conf. Comput. Vis. (ICCV)*, Dec. 2015, pp. 1440–1448.
- [29] X. Li, L. Li, F. Flohr, J. Wang, H. Xiong, M. Bernhard, S. Pan, D. M. Gavrilu, and K. Li, "A unified framework for concurrent pedestrian and cyclist detection," *IEEE Trans. Intell. Transp. Syst.*, vol. 18, no. 2, pp. 269–281, Feb. 2017, doi: [10.1109/TITS.2016.2567418](https://doi.org/10.1109/TITS.2016.2567418).
- [30] K. F. Wang, C. Gou, Y. J. Duan, Y. L. Lin, X. H. Zheng, and F. Y. Wang, "Generative adversarial networks: The state of the art and beyond," *Acta Automatica Sinica*, vol. 43, no. 3, pp. 321–332, 2017, doi: [10.16383/j.aas.2017.y000003](https://doi.org/10.16383/j.aas.2017.y000003).
- [31] K. Wang, C. Gou, Y. Duan, Y. Lin, X. Zheng, and F.-Y. Wang, "Generative adversarial networks: Introduction and outlook," *IEEE/CAA J. Automatica Sinica*, vol. 4, no. 4, pp. 588–598, 2017.
- [32] J. Wang, L. Gou, H. Yang, and H.-W. Shen, "GANViz: A visual analytics approach to understand the adversarial game," *IEEE Trans. Vis. Comput. Graphics*, vol. 24, no. 6, pp. 1905–1917, Jun. 2018, doi: [10.1109/TVCG.2018.2816223](https://doi.org/10.1109/TVCG.2018.2816223).
- [33] Q. B. Zhang, X. H. Zhang, and H. W. Han, "Back scattered light repairing method for under water laser image based on improved generative adversarial network," *Laser Optoelectron. Prog.*, vol. 56, no. 4, pp. 114–122, 2019.
- [34] C. Wang, C. Xu, X. Yao, and D. Tao, "Evolutionary generative adversarial networks," *IEEE Trans. Evol. Comput.*, vol. 23, no. 6, pp. 921–934, Dec. 2019, doi: [10.1109/TEVC.2019.2895748](https://doi.org/10.1109/TEVC.2019.2895748).
- [35] X. L. Tang, Y. M. Du, Y. W. Liu, J. Y. Li, and Y. W. Ma, "Image recognition with conditional deep convolutional generative adversarial networks," *Acta Automatica Sinica*, vol. 44, no. 5, pp. 855–864, 2018, doi: [10.16383/j.aas.2018.c170470](https://doi.org/10.16383/j.aas.2018.c170470).
- [36] Z. Zhong, J. Li, D. A. Clausi, and A. Wong, "Generative adversarial networks and conditional random fields for hyperspectral image classification," *IEEE Trans. Cybern.*, vol. 50, no. 7, pp. 3318–3329, Jul. 2020, doi: [10.1109/TCYB.2019.2915094](https://doi.org/10.1109/TCYB.2019.2915094).
- [37] K. Sheng, Z. Liu, D. C. Zhou, Q. H. Wei, and C. X. Feng, "A multi-class semi-supervised classification algorithm based on evidence theory," *Acta Electronica Sinica*, vol. 46, no. 11, pp. 2642–2649, 2018.
- [38] H. Zhao, Y. Xiao, and Z. Zhang, "Robust semisupervised generative adversarial networks for speech emotion recognition via distribution smoothness," *IEEE Access*, vol. 8, pp. 106889–106900, 2020, doi: [10.1109/ACCESS.2020.3000751](https://doi.org/10.1109/ACCESS.2020.3000751).
- [39] I. J. Goodfellow, "Generative adversarial networks," in *Proc. Adv. Neural Inf. Process. Syst.*, 2014, no. 3, pp. 2672–2680.
- [40] G. B. Kshirsagar and N. D. Londhe, "Improving Performance of Devanagari Script Input-Based P300 Speller Using Deep Learning," *IEEE Trans. bio-medical Eng.*, vol. 66, no. 11, pp. 2992–3005, Nov. 2019, doi: [10.1109/TBME.2018.2875024](https://doi.org/10.1109/TBME.2018.2875024).
- [41] C. A. Moreira, E. A. Philot, A. N. Lima, and A. L. Scott, "Predicting regions prone to protein aggregation based on SVM algorithm," *Appl. Math. Comput.*, vol. 359, pp. 502–511, Oct. 2019, doi: [10.1016/j.amc.2019.04.015](https://doi.org/10.1016/j.amc.2019.04.015).
- [42] T. Mo and P. Sun, "Research on key issues of gesture recognition for artificial intelligence," *Soft Comput.*, vol. 24, no. 8, pp. 5795–5803, Apr. 2020, doi: [10.1007/s00500-019-04342-3](https://doi.org/10.1007/s00500-019-04342-3).



**XINGANG JU** was born in August 1973. He graduated from Zhengzhou University in 2010. He received the master's degree in physical electronics from Zhengzhou University, in 2010, and the Ph.D. degree from the Henan Food Crop Collaborative Innovation Center, in 2014. As an Associate Professor since 2010, his research interests include quantitative analysis of terahertz time-domain spectroscopy and the application of THz-TDS to the detection of food quality.



**YUYING JIANG** was born in January 1984. She received the Ph.D. degree in information and signal processing from the University of Chinese Academy of Sciences, in 2016. Her research interests include the detection of the quality of stored grains with THz technology and spectral analysis, machine learning, and signal and information processing.



**FEIYU LIAN** was born in July 1970. He received the B.S. degree in information and communication engineering from Zhengzhou University, in 2001, and the Ph.D. degree in computer application technology from Shanghai University, in 2012. Since 2002, he has been a Lecturer with the Henan University of Technology, Zhengzhou, China. His research interests include quantitative analysis of terahertz time-domain spectroscopy and the application of THz-TDS to the detection of food quality.



**YUAN ZHANG** was born in May 1961. He received the bachelor's degree in automatic control from the University of Science and Technology of China, in 1983, and the Ph.D. degree in fuze technology from the Nanjing University of Science and Technology, in 1996. He is currently a Professor with the Henan University of Technology. He has authored or coauthored over 80 refereed journal and conference papers. His research interests include automatic control, machine learning, and signal and information processing.



**HONGYI GE** was born in July 1983. He received the Ph.D. degree in physical electronics from the University of Chinese Academy of Sciences, in 2015. He is currently an Associate Professor with the School of Computer Sciences and Technology, Henan University of Technology. He is also working on research of THz-TDS, THz imaging, deep learning, and image processing.



**DEGANG XU** was born in 1978. He received the B.S. degree in computer science from the Henan University of Science and Technology, in 2002, and the Ph.D. degree in systems engineering from the Huazhong University of Science and Technology, in 2011. He is currently an Associate Professor with the Henan University of Technology. His research interests include systems engineering of logistics, machine learning, image processing, and intelligent optimization algorithms.

...